Appl. Phys. A (2017) 123:422
DOI 10.1007/s00339-017-1026-y

Applied Physics A
Materials Science & Processing

Impedance and modulus spectroscopy of poly(vinyl alcohol)-$Mg[ClO_4]_2$ salt hybrid films

Reda Khalil[1]

Received: 29 November 2016 / Accepted: 8 May 2017 / Published online: 18 May 2017

Abstract The electrical and dielectric properties of PVA/$Mg[ClO_4]_2$ hybrid films were investigated in the temperature range of 90–150 °C and the frequency range of 20 Hz–10 MHz using impedance and modulus spectroscopy. Impedance and modulus analyses had indicated the temperature independent distribution of relaxation times and the non-Debye behavior in these composites. The co-operative motion due to strong coupling between the mobile Mg^{2+} ions is assumed to give rise to non-Debye type of relaxation. Complex impedance Nyquist plots are used to interpret the relaxation mechanism. The nature of Nyquist plot confirms the presence of bulk effects, grain boundaries and electrolyte/electrode polarization, and non-Debye type of relaxation processes occurs in the composites. A thermally activated relaxation was observed, which was ascribed to be a non-Debye-type relaxation caused by the mobility of magnesium ion in polymer matrix. A comparison between Z'', imaginary part of complex impedance, and M'', imaginary part of complex electric modulus, indicates that the short- and long-range charge motion dominates at low and high temperatures, respectively. The activation energies, which were obtained from the electric modulus and bulk conductivity, are matched well. The non-coincidence of peaks corresponding to the modulus and impedance indicates deviation from Debye-type relaxation.

✉ Reda Khalil
r.khalil@fsc.bu.edu.eg

[1] Physics Department, Faculty of Science, Benha University, Benha, Egypt

1 Introduction

Solid polymer electrolyte (SPE) composites are active materials, which provide an ideal solution to combine between their electrical properties and the application of electronic and optoelectronic devices [1–7]. Strong efforts are being made to find a suitable material with a high ionic conductivity of low-cost materials. The polymers, such as poly(methyl methacrylate), poly(styrene), poly(vinyl pyrrolidone), or poly(vinyl alcohol) (PVA), are unlikely to be useful as solid electrolyte materials due to their poor electrical conductivity and device stability. Several methods are used to improve the conductivity of polymer composites, such as copolymerization [8], plasticization [9], blending [10], and addition of fillers/inorganic salts [11–13]. Poly(-vinyl alcohol) is successfully used in a wide range of industrial field due to its excellent optical and electrical properties: good transparency, high dielectric strength, and fast charge transfer at electrode/electrolyte interface. The salts, which have polarizing cation and a large anion with a well-delocalized charge and low lattice energy, are suitable for use in solid polymer composites. Polymer electrolyte with magnesium ion conductor has recently found global interest due to high energy density and environmentally friendly components, coupled with low cost as alternative lithium electrolyte [14–18]. Ionic salts of $Mg[ClO_4]_2$ are well known as potential candidate for batteries and fuel cell membranes because of its large specific capacitance.

It is important to understand the ion transport and relaxation mechanisms in these composite polymer electrolytes. The complex impedance spectroscopy is the powerful experimental tools. It can be used to investigate the correlation between the microstructure and electrical relaxations [19] and may find the generalization of relaxation processes.

The impedance and electrical modulus spectroscopy are crucial quantities required to understand interaction between the polymer host and dopant salt. They also give us information about the nature and types of molecular motions. They are affected by chemical composition, temperature, and/or frequency [20, 21]. One advantage of dielectric behavior study is that helps in investigating the conductive behavior of polymer electrolyte. Modulus spectroscopy is known as a "good" dielectric function in revealing the hidden dielectric relaxations [22].

SPEs are interesting to study not only from the fundamental understanding of ion transport in polymers but also from their possible applications in various electrochemical devices [23–25]. It is well known that SPEs differ from usually glassy ion conductors in the structure. In general, polymer electrolytes are in rubber-like state, whereas the glass conductors are in "glass-like" state at room temperature. This means that the mobile ions hop between fixed vacant sites in glass and movable vacant sites in polymer composites giving rise to the conductivity. The ionic conductivity in SPEs takes place in the amorphous phase, where the ion conduction is mediated by local motion of the polymer chain segments and different mobile ions (ion atmosphere). The latter leads to either ion ordering or formation of more dynamical structures. Therefore, the segmental mobility plays a critical role in ion transport behavior in polymer electrolyte [24, 25]. Therefore, it becomes important to understand the ion transport mechanism along with polymer segmental relaxation processes in polymer electrolytes.

In view of the importance of ac impedance analysis, the present work aims to study the effect of Mg salt content on the electrical and dielectric behavior of the PVA/$Mg[ClO_4]_2$ SPEs. Detailed magnesium ion dynamics and segmental relaxation of PVA/Mg salt electrolyte complex have been analyzed by the impedance data as a function of frequency at varying temperatures. However, the relaxation times of the physical processes themselves cannot be obtained directly if their impedance contributions have distribution of relaxation times, non-Debye model. Equivalent circuit model is obtained by means of complex nonlinear least squares (CNLS) fitting and finally establishes a deeply comprehensive visualize about the physics and dynamics of these kind of devices.

The dielectric properties are discussed and correlated with the microstructure properties. The loading concentration of $Mg[ClO_4]_2$ salt in the polymer was found to have a significant influence on the dielectric properties. This can be best understood by combining impedance and modulus formalisms.

2 Experiments

The solid polymer electrolyte films of pure and magnesium perchlorate-doped PVA were prepared by weight percent ratios (90:10), (80:20), (70:30), and (60:40) by solution cast technique using distilled water as a solvent. The more details of sample preparation have been described elsewhere [26].

The impedance measurements were performed using Gwinstek LCR-811OG high precision impedance analyzer interfaced to a computer in the frequency range from 20 Hz to 10 MHz and in the temperature range of 90–150 °C. Samples were mounted on the conductivity holder with stainless steel electrodes under spring pressure.

The data of impedance may be analyzed in terms of two possible complex formalisms: the impedance Z^* and the electrical modulus M^*. These parameters are related according to the expressions [27, 28]:

$$\text{Complex impedance } Z^* = Z' - jZ'' = \frac{1}{j\omega\varepsilon_o\varepsilon^*} \quad (1)$$

$$\text{Complex Modulus } M^* = M' - jM'' = \frac{1}{\varepsilon^*} = \frac{\varepsilon' + j\varepsilon''}{(\varepsilon')^2 + (\varepsilon'')^2}, \quad (2)$$

where ω is the angular frequency and ε_o is the vacuum capacitance of the measuring cell. The use of the formula of M^* is convenient to the resistive and/or capacitive analysis when localized relaxation dominates, while the Z^* formula is favorable when the long-range conductivity dominates. In particular, the use of Z^* formalism allows for a direct separation of the bulk and bulk/electrode interface phenomena [29]. The impedance spectra were analyzed by equivalent circuit modeling using the complex nonlinear least squares fitting procedure (CNLS). CNLS fitting was performed by means of the program EIS spectrum analyzer which is available free of charge via the internet.

3 Results and discussion

To get better understanding on the dielectric relaxation behaviors of PVA/magnesium salt, the impedance and electrical modulus spectra of the sample have been studied. Figure 1a shows the variation of the imaginary part (Z'') of the complex impedance (Z^*) as a function of frequency (f) for SPE $[PVA]_{90}$-$[Mg[ClO_4]_2]_{10}$ as a representative sample. The spectrum is characterized by the appearance of a peak at a frequency which is conventionally known as the "relaxation frequency" (f_{max}). In addition, when the temperature increases, the peak amplitude and peak broadening of Z'' decrease and the peak position shifts to the higher frequencies. These features indicate that the relaxation

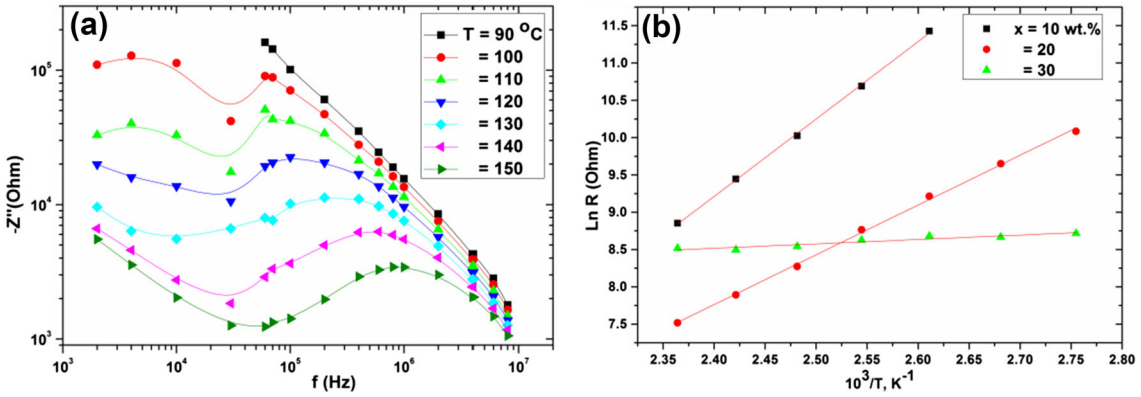

Fig. 1 **a** Spectroscopic plots of the impedance (Z'') obtained versus frequency at various temperatures for SPE $[PVA]_{90}$-$[Mg[ClO_4]_2]_{10}$ as a representative sample and **b** Arrhenius plot for resistance, which was calculated from Z'' peak

times (τ) are not a single valued, but it is distributed continuously [19] and thermally activated [30], respectively.

Since the Z'' (ω) peak reaches its crest with the value of $Z'' = R/2$ (see [19]), we can easily deduce the resistance at different temperatures and plot it against the reciprocal of temperature, as shown in Fig. 1b. It was shown that the resistance obeys the Arrhenius relation:

$$R = R_o \exp\left(\frac{E_{cond.}}{k_B T}\right), \quad (3)$$

where R_o, $E_{cond.}$, k_B and T are the pre-exponential term, activation energy of conduction, Boltzmann constant, and the absolute temperature, respectively. Linear fitting for samples with different Mg salt concentrations, $x = 10$, 20 and 30 wt%, gives $E_{cond} = 0.894$, 0.575 and 0.051 eV, respectively. It is noted that the activation energy of the conduction is decreased with increasing the magnesium salt concentration. It also noticed from Fig. 1b that the resistivity of the sample 30 wt% is higher than the sample 20 wt% at higher temperature range (120–150 °C). It has been argued that mobile ion concentration can be reduced by the segregation of the Mg salt in polymer matrix. The surface morphology of the SPE composite polymer films shows lumps of Mg salt on the top surface [26]. These lumps embedded in the polymer matrix. When the Mg salt content is increased, the composites showed a dispersion problem with agglomeration of Mg salt up to 30 wt%. The compatibility of the PVA matrix with lumps is completely uniform dissolved and homogenous when the Mg salt content is 40 wt%. Therefore, it is suggested that the lumps sized Mg salt prevents local PVA chain reorganization with the result of locking in at higher temperature a low degree of disorder characteristic of the amorphous phase, which in turn favors high ionic transport.

Moreover, the full-width at half-maxima (FWHM) calculated from the impedance loss spectra (log [Z'' versus f]) are greater than 1.144 decades, ideal Debye relaxation, which deviates from Debye-type relaxation [31]. This deviation from ideal Debye relaxation might be due to an implicit non-exponential process, such as correlation between diffusive motion of the charge carriers and electrical response time [32, 33]. In addition, the Z'' curves at all temperatures merge together at high frequency, which indicates a possible release of the free volume. Therefore, the high-frequency dielectric response is dominated by the electrical response within the magnesium salt particles.

The Nyquist plot obtained by plotting Z'' versus Z' will exhibit a semicircle with diameter representing the bulk resistance R_b of the sample when a dielectric relaxation occurs [31] (see Fig. 2). The Nyquist plot shows a semicircular at high frequency and spike at low frequency. The semicircle diameter is decreased and the spike is elongated with increasing the temperature and/or the concentration of magnesium salt. The tail can be easily ascribed to the interface of the electrolyte/electrode contact. All the semicircles exhibit some depression instead of a semicircle centered on real axis Z' due to a distribution of relaxation times. The result indicates that the relaxation is an ideal non-Debye-type relaxation contributed by bulk response.

To investigate quantitatively of the impedance data and establish a connection between microstructure and electrical properties, experimental data are usually modeled by an ideal equivalent electrical circuit fitting. For the fitting of the impedance data, the use of constant phase elements (CPEs) was important. A CPE is an equivalent electrical circuit component that models the behavior of an imperfect capacitor. The impedance of the CPE is defined as $Z_{CPE} = \frac{1}{Q(i\omega)^n}$, where Q is the numerical value of $|Z|^{-1}$ at $\omega = 1$ rad s^{-1} and n is the phase of the elements. The CPE acts as a pure capacitor and pure resistor when $n = 1$ and 0, respectively. The experimental data were fitted using the EIS software and the solid lines in Fig. 2 represent the fitting results of the equivalent circuit model. The very good agreement between the data and the modeling results

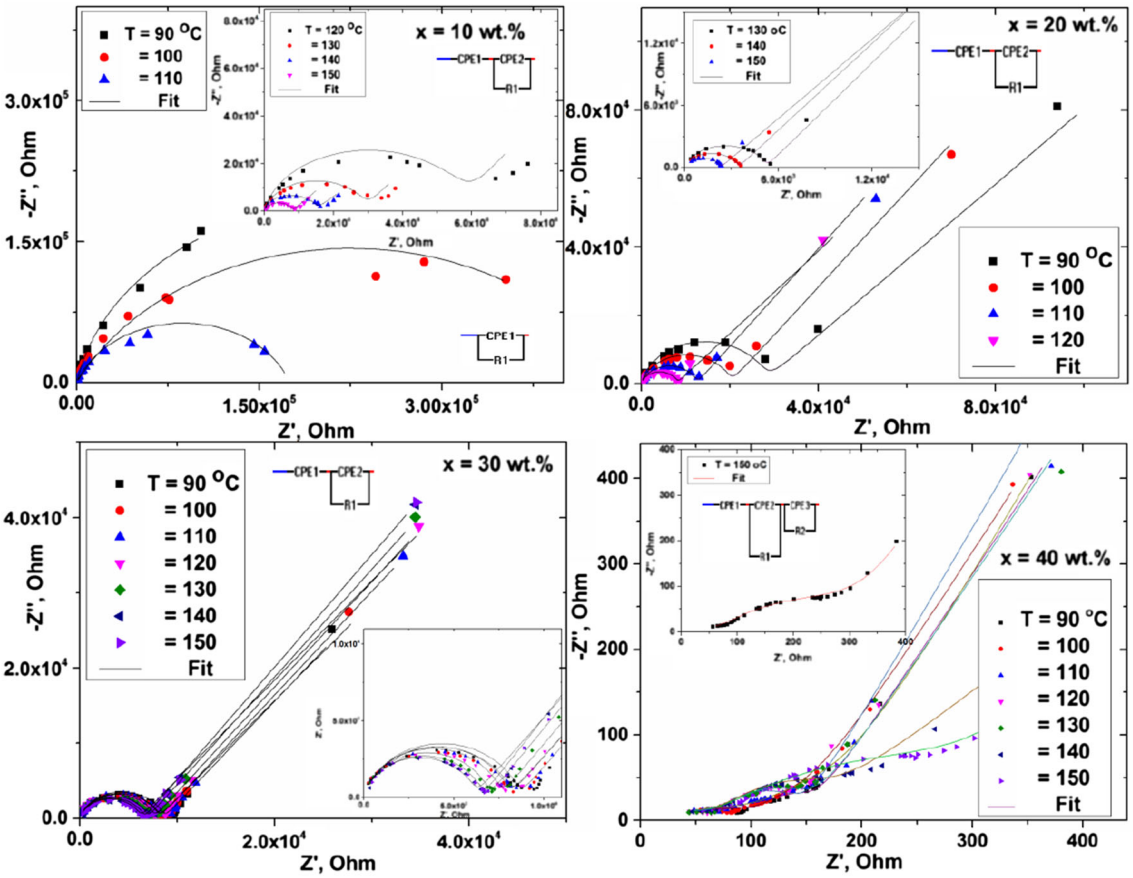

Fig. 2 Nyquist plots of various magnesium salt contents of SPE samples in PVA/$Mg[ClO_4]_2$ system (*asterisks* are the experimental points, and the *solid line* represents the result of fitting)

Table 1 Summarizing of fitting parameters corresponding to equivalent circuit model at 130 °C of Fig. 2

Mg salt wt%	Fitting parameters							
	R_1, (kΩ)	Q_1, μF	n_1	Q_2, F	n_2	R_2, (Ω)	Q_3, μF	n_3
10	28.5	0.21	0.624	7.8×10^{-11}	0.904			
20	05.2	1.2	0.623	1.8×10^{-10}	0.859			
30	06.9	1.1	0.612	9.8×10^{-11}	0.888			
40	0.06	23	0.739	7.1×10^{-5}	0.280	188.83	0.28	0.885

confirms that the selected equivalent circuit is an appropriate choice. The individual variables obtained from the fit are depicted in Table 1. The circuit, which is used for fitting, is shown in the inset of Fig. 2.

To explore more information about which kind of dielectric charge species that causes the relaxation, we resort to the dielectric function of the electric modulus. Ionically conducting materials are also investigated using complex electric modulus formalism [34]. The electric modulus, $M^*(\omega)$, is defined in terms of complex dielectric permittivity, $\varepsilon^*(\omega)$, as shown in Eq. (2). This scaling formalism is notably suitable to detect and distinguish between the electrode polarization phenomenon and bulk effects as average conductivity relaxation times τ [35].

Figure 3 displays the spectroscopic plots of the imaginary part of the electric modulus for PVA/$Mg[ClO_4]_2$ electrolyte at temperatures varying from 90 to 150 °C and frequency range from 20 Hz to 10 MHz. The values of the imaginary part of the electric modulus approach almost zero at low frequencies, which indicate that the electrode polarization has negligible contribution. Figure 3 also shows an asymmetric shape spectrum behavior with respect to M'' peak and this peak shifts towards higher frequency as the temperature increases, which indicates of the thermally activated relaxation.

Two apparent relaxation regions appear above and below M''_{max}. The region on behalf of left of the peak is associated with the conduction process, where the charge

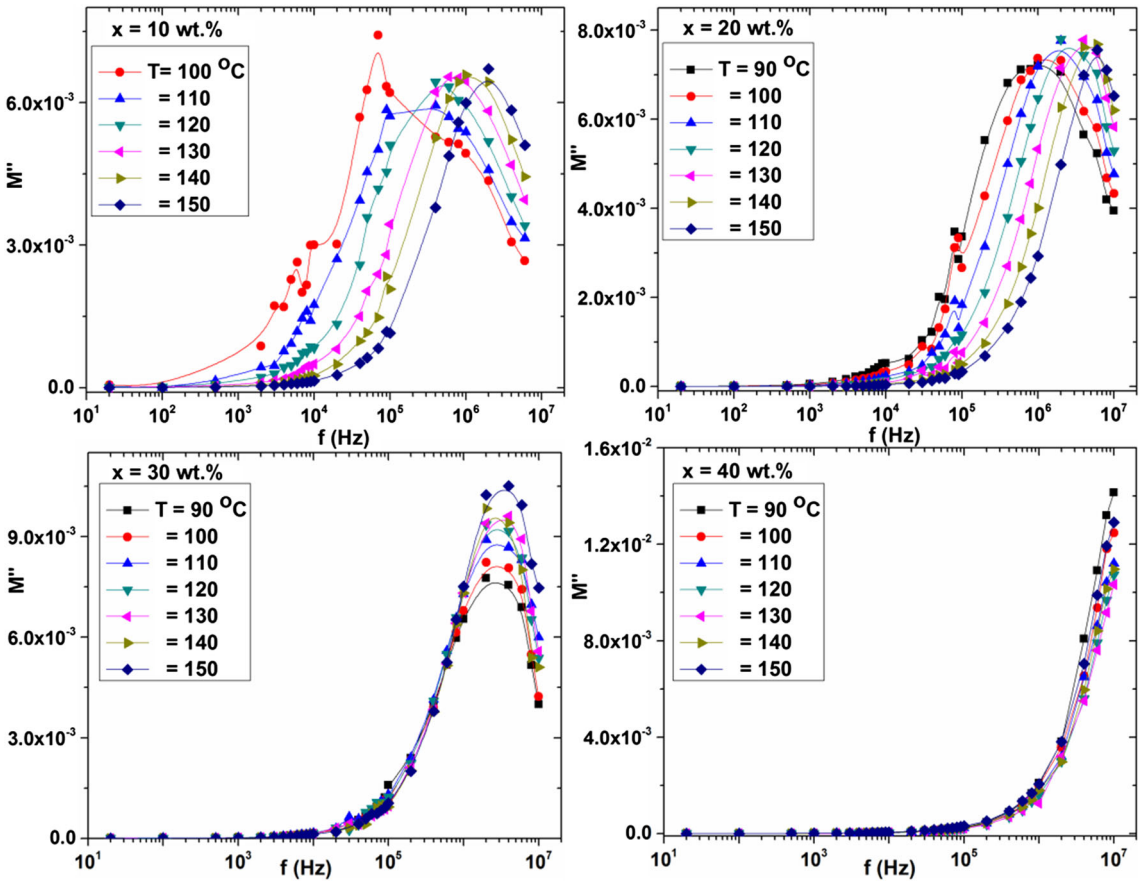

Fig. 3 Spectroscopic plots of the electric modulus (M'') for SPE PVA/$Mg[ClO_4]_2$ sample obtained at various temperatures

carriers are mobile over a long distance. However, the region on behalf of right of the peak is associated with the relaxation polarization process, where the charge carriers are spatially confined to the potential wells (localized) [36]. Thus, the peak frequency is indicative of transition from long-range to short-range mobilities. Relaxation parameter analysis is favorable for better understanding of the physical nature of the observed relaxation, which can be obtained in terms of the Arrhenius law:

$$f_p = f_o \exp\left(\frac{-E_{rela}}{k_B T}\right), \quad (4)$$

where f_p is the frequency, the maximum M'' (f) occurs, f_o is the pre-exponential factor, and E_{rela} is the activation energy of the relaxation. The values of f_o and E_{rela} for samples $x = 10$, 20, and 30 wt%, which were obtained from the Arrhenius plot (see Fig. 4), are 2.1×10^{16}, 1.0×10^{15}, and 2.28×10^{7} Hz and 0.839, 0.719, and 0.068 eV, respectively. We notice that the activation energies of the relaxation are decreased with increasing the magnesium salt in polymer matrix. These values are very close to the activation energy for dc conduction [13], which indicates that the ionic migration is responsible for the observed dc

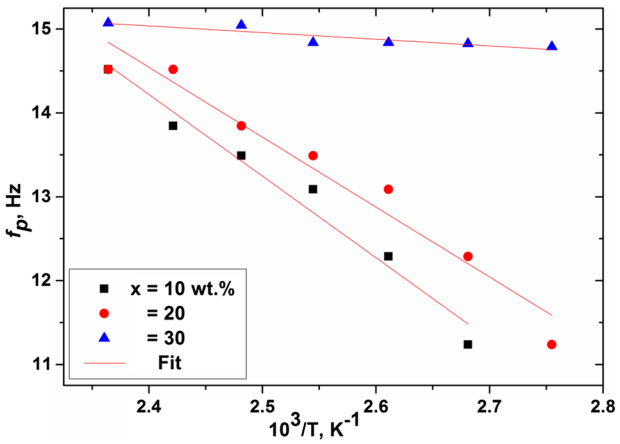

Fig. 4 Arrhenius plot for the frequency, f_p, at M'' peak for SPE PVA/$Mg[ClO_4]_2$

conductivity and modulus spectrum, further convincing that both aspects are strongly related [37].

Figure 5a illustrates the plot between M/M_{max} and log (f/f_{max}) at different temperatures for $[PVA]_{80}$-$[Mg[ClO_4]_2]_{20}$ solid polymer electrolyte as a representative sample. This is called the master electric modulus curve and it gives an insight into the dielectric processes occurring inside the

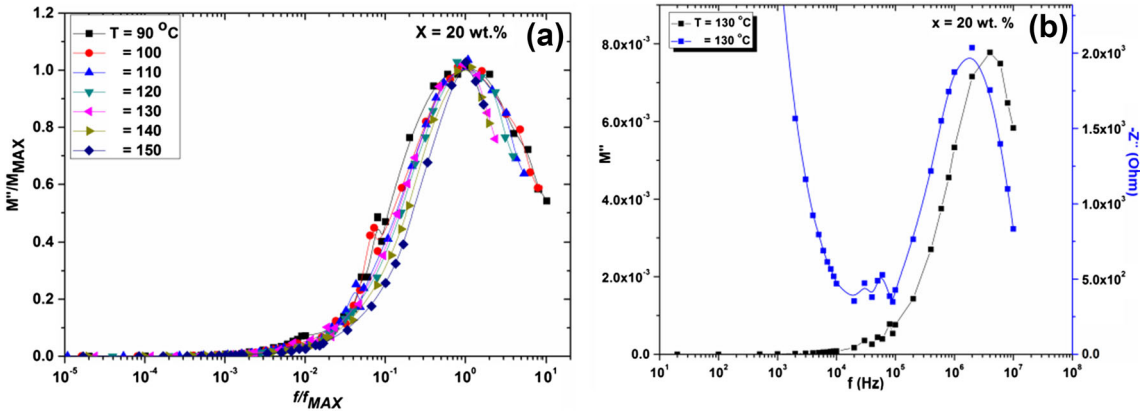

Fig. 5 **a** Scaled imaginary part of electric modulus M''/M''_{max} versus log f/f_{max} and **b** imaginary part of impedance (Z'') and imaginary part of modulus (M'') as a function of frequency at 130 °C for $[PVA]_{80}$-$[(Mg[ClO_4]_2]_{20}$ SPE as representative sample

material. These plots overlap on a single master curve indicating that the distribution of relaxation time is independent of temperature [38, 39]. This means that the conduction mechanism remains unchanged and it is also indicative of a common ion transport mechanism. Therefore, the relaxation can be reasonably ascribed to the hopping motion of magnesium ions.

Figure 5b shows the frequency response of Z'' and M'' of Mg salt in polymer at temperature $T = 130$ °C for $[PVA]_{80}$-$[Mg[ClO_4]_2]_{20}$ SPE. The peaks of both impedance and modulus plots should coincide in the Debye-type relaxation. Any departure from this behavior is non-Debye-type relaxation. From this plot, the Z'' and M'' peaks do not coincide, which indicate non-Debye relaxation for this sample. The advantages of the combined Z'' and M'' graph is to distinguish whether a particular relaxation process in the material due to the long or short-range movement of charge carriers [40]. The non-coincidence of peaks corresponding to Z'' and M'' indicates the relaxation due to the short-range movement of charge carriers. The large rise in Z'' at low frequencies comes from the electrode polarization.

4 Conclusions

In conclusion, the electrical and dielectric properties of PVA-$Mg[ClO_4]_2$ hybrid films were investigated in the temperature range of 90–150 °C and the frequency range of 20 Hz–10 MHz using impedance and electrical modulus spectroscopy. PVA-$Mg[ClO_4]_2$ SPEs were observed a thermally activated relaxation. Our results obtained indicate that the relaxation is caused by the hopping motion of magnesium ions. Complex impedance and complex electrical modulus formalism were used to study the frequency dependence of ion dynamics at different temperatures. The electrical modulus scaling study appreciates the merit of the present systems, and shows universal features of other reported SPEs. Dielectric relaxation studies have shown the presence of non-Debye-type dielectric relaxation in this material.

References

1. M. Bajpai, R. Srivastava, R. Dhar, R.S. Tiwari, S. Chand, Adv. Mater. Lett. **7**(5), 414 (2016)
2. J.H. Noh, S.H. Im, J.H. Heo, T.N. Mandal, S.I. Seok, Nano. Lett. **13**, 1764 (2013)
3. Z.S. Guo, L. Zhao, J. Pei, Z.L. Zhou, G. Gibson, J. Brug, S. Lam, S.S. Mao, Macromolecules **43**, 1860 (2010)
4. S. Coe-Sullivan, W.K. Woo, J.S. Steckel, M. Bawendi, V. Bulovi, Org. Electron. **4**, 123 (2003)
5. T.N. Smirnova, O.V. Sakhno, P.V. Yezhov, L.M. Kokhtych, L.M. Goldenberg, J. Stumpe, Nanotechnology **20**, 245707 (2009)
6. B.C. Das, A.J. Pal, ACS Nano. **2**, 1930 (2008)
7. A. Guchhait, A.K. Rath, A.J. Pal, Chem. Mater. **2**, 5292 (2009)
8. W. Wieczorek, Z. Florjanczyk, J.R. Steven, Electrochim. Acta **40**, 2251 (1995)
9. K. Nagoka, H. Naruse, I. Shinohara, M. Watanabe, J. Polym. Sci. Polym. Lett. **22**, 659 (1984)
10. F.F. Hatta, M.Z.A. Yahya, A.M.M. Ali, R.H.Y. Subban, M.K. Harun, A.A. Mohamed, Ionics **11**, 418 (2005)
11. I.S. Noor, S.R. Majid, A.K. Arof, Electrochim. Acta **102**, 149 (2013)
12. K.S. Hemalatha, G. Sriprakash, M.V.N. Ambika Prasad, R. Damle, K. Rukmani, J. Appl. Phys. **118**, 154103 (2015)
13. R. Khalil, E. Sheha, T. Hanafy, O. Al-Hartomy, Mater. Express **4**, 483 (2014)
14. T.D. Gregory, R.J. Hoffman, R.C. Winterton, J. Electrochem. Soc. **137**, 775 (1990)
15. M. Vittadello, S. Biscazzo, S. Lavina, M. Fauri, V. Di Noto, Solid State Ion. **147**, 341 (2002)
16. D. Aurbach, Z. Lu, A. Schechter, Y. Gofer, H. Gizbar, R. Turgeman, Y. Cohen, M. Moshkovich, E. Levi, Nature **407**, 724 (2000)
17. D. Aurbach, Y. Gofer, Z. Lu, A. Schechter, O. Chusid, H. Gizbar, Y. Cohen, V. Ashkenazi, M. Moshkovich, R. Turgeman, E. Levi, J. Power Sour **97–98**, 28 (2001)
18. J. Muldoon, C.B. Bucur, A.G. Oliver, T. Sugimoto, M. Matsui, H.S. Kim, G.D. Allred, J. Zajicek, Y. Kotani, Energy Environ. Sci. **5**, 5941 (2012)

19. J.R. Macdonald, *Impedance spectroscopy: emphasizing solid materials and systems* (Wiley, New York, 1987)
20. Y. Shao, N.N. Rajput, J. Hu, M. Hu, T. Liu, Z. Wei, M. Gu, X. Deng, S. Xu, K.S. Han, J. Wang, Z. Nie, G. Li, K.R. Zavadil, J. Xiao, C. Wang, W.A. Henderson, J. Zhang, Y. Wang, K.T. Mueller, K. Persson, J. Liu, Nano Energy **12**, 750 (2015)
21. G.P. Pandey, R.C. Agrawal, S.A. Hashmi, J. Solid State Electrochem. **15**, 2253 (2011)
22. C.C. Wang, J. Wang, X.H. Sun, L.N. Liu, J. Zhang, J. Zheng, C. Cheng, Solid State Commun. **179**, 29 (2014)
23. J.R. Maccallum, C.A. Vincent (eds.), *Polymer electrolyte review I and II* (Elsevier, London, 1987)
24. W.H. Meyer, Adv. Mater. **10**, 439 (1998)
25. F.M. Gray, *Polymer electrolyte*, Chap 2 (The RSC Materials Monographs, London, 1997)
26. R. Khalil, E.M. Sheha, A. Eid, J. Adv. Phys. **6**, 102 (2017)
27. F.S. Howell, R.A. Bose, P.B. Macedo, C.T. Moynihan, J. Phys. Chem. **78**, 639 (1974)
28. K. Yamamoto, H. Namikawa, Jpn. J. Appl. Phys. **27**, 1845 (1988)
29. D.C. Sinclair, A.R. West, J. Appl. Phys. **66**, 3850 (1989)
30. R. Sathiyamoorthi, P. Shakkthivel, S. Ramalakshmi, Y.G. Shul, J. Power Sour. **171**, 922 (2007)
31. N. Ortega, A. Kumar, P. Bhattacharya, S.B. Majumder, R.S. Katiyar, Phys. Rev. B **77**, 014111 (2008)
32. J. Liu, C.G. Duan, W.G. Yin, W.N. Mei, R.W. Smith, J.R. Hardy, Phys. Rev. B **70**, 144106 (2004)
33. C.T. Moynihan, Solid State Ion. **105**, 175 (1998)
34. I.M. Hodge, M.D. Ingram, A.R. West, J. Electroanal. Chem. Interfacial Electrochem. **74**, 125 (1976)
35. R. Gerhardt, J. Phys. Chem. Solids **55**, 1491 (1994)
36. S. Lanfredi, P.S. Saia, R. Lebullenger, A.C. Hernandes, Solids State Ion. **146**, 329 (2002)
37. M. Sural, A. Ghosh, Solid State Ion. **130**, 259 (2000)
38. D.P. Almond, A.R. West, Solid State Ion. **9**, 277 (1983)
39. D.P. Almond, A.R. West, Solid State Ion. **23**, 27 (1987)
40. W. Cao, R. Gerhardt, Solid State Ion. **42**, 213 (1990)